

In vivo estimation of the photosystem II photochemical efficiency of individual microphytobenthic cells using high-resolution imaging of chlorophyll *a* fluorescence

Abstract—Rates of primary production by intertidal microphytobenthos within biofilms have been shown to be very high. An essential step toward assessing the contribution of individual species to this level of production is the in vivo measurement of photosynthetic efficiency from individual cells. A strong relationship between photosystem II photochemical efficiency and the fluorescence parameter F_q'/F_m' (where $F_q' = F_m' - F'$) has been established within higher plants and unicellular algae. Calculation of F_q'/F_m' requires measurement under constant light (at the F' level of fluorescence) and during a pulse of saturating light (at the F_m' level of fluorescence). High-resolution imaging of chlorophyll fluorescence at the F' and F_m' levels has allowed the construction of F_q'/F_m' images from individual cells of several species of diatom and *Euglena* sp. within intact biofilms. No species differences in the values of F_q'/F_m' were observed at low levels of incident light. However, *Euglena* sp. showed significantly higher F_q'/F_m' values at moderate to high incident light levels than all of the diatom species. Endogenous rhythms of vertical migration during tidal exposure and peaks in photosystem II photochemical efficiency at low tide could also be followed using this technique. Clear differences were observed in the migration of individual taxa to the surface of the biofilm. Images of F_q'/F_m' were also used to assess the scale of heterogeneity for this parameter. Overall, these data demonstrate that high-resolution imaging of chlorophyll fluorescence is a valuable technique that allows for determination of the photosystem II photochemical efficiency from different microphytobenthic taxa within biofilms.

Microphytobenthos are the dominant primary producers within cohesive intertidal and shallow subtidal sediment habitats. Estimates of microphytobenthic primary production range from 30 to 230 g C m⁻² yr⁻¹ (MacIntire et al. 1996; Underwood and Kromkamp 1999), a figure that represents approximately 50% of the primary productivity of some estuarine regions (Underwood and Kromkamp 1999). Microphytobenthos also play an important role in the stabilization of sediments, primarily through formation of biofilm structures that results from production of exopolymers (Paterson 1989; Smith and Underwood 1998).

Despite the importance of biofilms to the ecology and dynamics of intertidal systems, our understanding of the physiology of microphytobenthos is relatively poor. The composition of biofilms is also known to change rapidly in response to factors such as temperature, salinity, nutrients, high light, and ultraviolet B (UVB; Blanchard et al. 1996; Barranguet et al. 1998; Underwood et al. 1998, 1999). Biofilm species composition varies throughout the annual cycle (Underwood and Kromkamp 1999) and changes in species composition have been suggested to explain differences in photosynthetic performance (Blanchard et al. 1996; Kromkamp et al. 1998).

Data from a number of studies indicate that conventional

(integrated) modulated fluorometry allows for the rapid and reproducible measurement of meaningful fluorescence parameters, in situ and in vivo (i.e., within intact biofilms), at temporal and spatial scales that are relevant to microphytobenthic ecology (Serôdio et al. 1997; Hartig et al. 1998; Kromkamp et al. 1998; Underwood et al. 1999). This is in contrast to studies using microelectrodes, where adequate replication within a short time period is problematic, and ¹⁴C and oxygen exchange techniques that require long incubations and involve substantial alteration of environmental conditions (Underwood and Kromkamp 1999).

Modulated chlorophyll fluorometry has been widely used to investigate photochemical activity within higher plants. For useful information to be retrieved, it is normally necessary to measure the fluorescence signal under constant light (F_o or F' in the dark- and light-adapted states, respectively) and the maximum level of chlorophyll fluorescence (F_m or F_m' in the dark- and light-adapted states, respectively), which has been achieved here by the application of saturating, multiple turnover pulses. The fluorescence parameter F_q'/F_m' (where $F_q' = F_m' - F'$) is of particular value, because it is theoretically proportional to the yield of photosystem II (PS II) photochemistry and has frequently been shown to have a strong, quantitative relationship with the quantum yield of CO₂ assimilation (ϕ_{CO_2}) (Genty et al. 1989; Di Marco et al. 1990; Krall and Edwards 1990; Edwards and Baker 1993). Significant correlations between the apparent efficiency of PS II photochemistry (estimated from chlorophyll fluorescence) and the yield of O₂ evolution have also been observed in both phytoplankton (Falkowski et al. 1991; Kolber and Falkowski 1993) and microphytobenthos (Hartig et al. 1998).

The species composition of microphytobenthic biofilms within the estuarine environment is known to vary both spatially and seasonally and also in response to various anthropogenic causes, such as organic pollution (Underwood 1994, 1997; Peletier 1996; Underwood et al. 1998). Though studies on single species in culture and sediment slurries (Blanchard et al. 1996; Hartig et al. 1998) have provided valuable data on the response of microphytobenthos to changing environmental conditions, the potential importance of light, nutrient, and CO₂ limitation in vivo can only be assessed through measurements on undisturbed biofilms at a scale appropriate to the processes concerned (Kromkamp et al. 1998). This type of investigation is complicated by the intimate relationship between the biofilm and substratum, including rapid attenuation of photosynthetically active photon flux density (PPFD) within the sediment that restricts the majority of photosynthesis to the top 200–400 μm, and the typically wide species diversity (Underwood and Kromkamp 1999).

The development of high-resolution chlorophyll fluorescence imaging, based around a fluorescence microscope (Ox-

borough and Baker 1997a,b), has allowed measurement of established fluorescence parameters at the subcellular level in higher plants. The main aim of this study was to evaluate this system as a noninvasive technique for determining the relative PS II photochemical efficiency of microphytobenthos on fine intertidal sediments. Fluorescence microscopy has been employed in estimation of the maximum photochemical efficiency at PS II within single cells of pelagic algae (Olson et al. 1996). However, this earlier system relied upon the isolation of a single cell within the field of view for each measurement and could not be used for estimation of the operating efficiency of PS II photochemistry (through F_q'/F_m') or for the simultaneous measurement of this parameter from a large number of cells.

In this study, chlorophyll fluorescence has been imaged at steady state (F') from individual cells within intact biofilms at PPFD values of between 60 and 800 $\mu\text{mol m}^{-2} \text{s}^{-1}$. Images were also taken at the F_m' level of fluorescence, during pulses of saturating light, within 2 s of each F' image. From these two images, plus appropriate corrective images (Oxborough and Baker 1997a), it was possible to construct images of F_q'/F_m' from natural sediment biofilms that had been subjected to minimal disturbance. It is possible to calculate values of F_q'/F_m' at the level of individual microphytobenthic cells with this system and, simultaneously, to follow the patterns of vertical migration of different taxa.

All of the images used in this study were taken using a 10 \times objective that provides a pixel resolution of (2.14 μm)² and covers an area of 0.82 mm \times 1.24 mm (1.02 mm²). Exposure times for images of F were between 1 s at a PPFD of 790 $\mu\text{mol m}^{-2} \text{s}^{-1}$ and 15 s at a PPFD of 60 $\mu\text{mol m}^{-2} \text{s}^{-1}$. Images of F_m' were taken over the last 250 ms of a 600-ms saturating pulse at 12,400 $\mu\text{mol m}^{-2} \text{s}^{-1}$. Using a computer program written specifically for use with this system, it was possible to construct an image of F_q'/F_m' and determine a mean value for this parameter within a few seconds of the end of the F_m' pulse. Consequently, changes in F_q'/F_m' could be followed in real time, ensuring that a steady-state rate of photosynthesis had been attained at each PPFD, where appropriate. Individual cells were isolated within images using editing tools built into the computer program (Fig. 1). In many instances, a small degree of cell movement occurred between imaging at F' and F_m' . This could usually be compensated for by using a nudging facility within the computer program (Fig. 1D). In this instance, the F_m' image (green pixels) was nudged up one pixel, which led to a marginal decrease in the range of pixel values within the final image of F_q'/F_m' (not shown), but no measurable change in the value of F_q'/F_m' .

Measurements were made on a number of samples of intertidal biofilms, collected during March and April 1998. The data presented in Figs. 2, 3, and 4 are from two such samples. The first was collected on 18 March 1998 from Colne Point, Essex, U.K. and imaged on 19 March 1998 (sample M19), while the second was collected Alresford Creek, Essex, U.K. on 1 April 1998 and imaged on 2 April 1998 (sample A02). Sampling occurred during daytime low tides and involved removing the top 1 cm of sediment using a flat metal plate and carefully placing it in a petri dish, ensuring minimal disturbance of the sediment surface. Sediment sam-

ples were maintained at in situ temperatures under natural illumination and imaging was undertaken during the subsequent daytime low tide period, in synchrony with the endogenous vertical migratory rhythm of the microphytobenthos.

Figure 2A and C are F_m' images from samples A02 and M19, respectively, taken once a steady state had been reached at a PPFD of 200 $\mu\text{mol m}^{-2} \text{s}^{-1}$ (after at least 30 min). The species composition of the surface assemblage of sample A02 was diatom rich, being composed of *Plagiotropis vitrea* (66%); small *Navicula*, predominantly *N. phyllepta* (Kütz.) and *N. flanatica* (Grun) (16%); *Pleurosigma angulatum* (7%); *Nitzschia sigma* (Kütz.) W. Smith (5%); *Gyrosigma littorale* (4%); and *Euglena* sp. (4%). Conversely, sample M19 was comparatively rich in *Euglena* sp., the overall composition being *Euglena* sp. (40%); *P. vitrea* (29%); *P. angulatum* (18%); *G. littorale* (3%); *Diploneis didyma* (Ehrenberg) Cleve (3%); and small *Navicula*, predominantly *N. phyllepta* and *N. flanatica* (3%). Figure 2B and D are false color images of F_q'/F_m' from the same areas of samples A02 and M19 as Fig. 2A and 2C, respectively.

To determine the level of variation within the images shown in Fig. 2, regions were isolated using quadrats of different sizes. The quadrat sizes used were 25 \times 25 pixels (2,862 μm^2), 50 \times 50 pixels (11,499 μm^2), 75 \times 75 pixels (25,760 μm^2), 100 \times 100 pixels (45,796 μm^2), and 150 \times 150 pixels (103,041 μm^2). Twelve independent quadrats of each size were placed at random locations within images. A single mean value for F_q'/F_m' within each quadrat was calculated using the sums of all values of F_m' and F' within each quadrat; i.e., as $(\sum F_m' - \sum F')/\sum F_m'$, rather than the mean of $\sum [(F_m' - F')/F_m']$ (Fig. 3A,B). Because the integrated means were calculated after summing all values within the F_m' and F' images, these measurements are analogous to those made by a conventional (integrating), modulated fluorometer. A second mean value was calculated for cells that could be isolated at the sediment surface within each quadrat (Fig. 3A,B). The coefficient of variation (CV) of F_q'/F_m' was calculated for each quadrat size; from both the integrated mean values and the cells isolated at the sediment surface (Fig. 3C,D). There were significant declines in the CV of F_q'/F_m' with increasing spatial scale for both types of biofilm and both types of mean values. The dependence of CV on quadrat size was most apparent with the mean values derived from cells isolated at the biofilm surface of sample M19. It is clear, from these data, that the variation within an image is unlikely to contribute, significantly, to the standard error about the mean of samples from different sites or different regions of the same site.

In sample A02, the integrated means of F_q'/F_m' were significantly higher than the means derived from cells isolated at the biofilm surface, at all quadrat sizes (ANOVA $P < 0.01$) (Fig. 3A). This observation is likely to be due to a significant fluorescence contribution from cells at depth, where values of F_q'/F_m' are likely to be lowered as the result of attenuation of incident PPFD by the sediment. In contrast to the data from sample A02, there was no measurable difference between the values of F_q'/F_m' from cells isolated at the biofilm surface of the *Euglena*-rich biofilm (sample M19) and integrated means from the whole film (Fig. 3B).

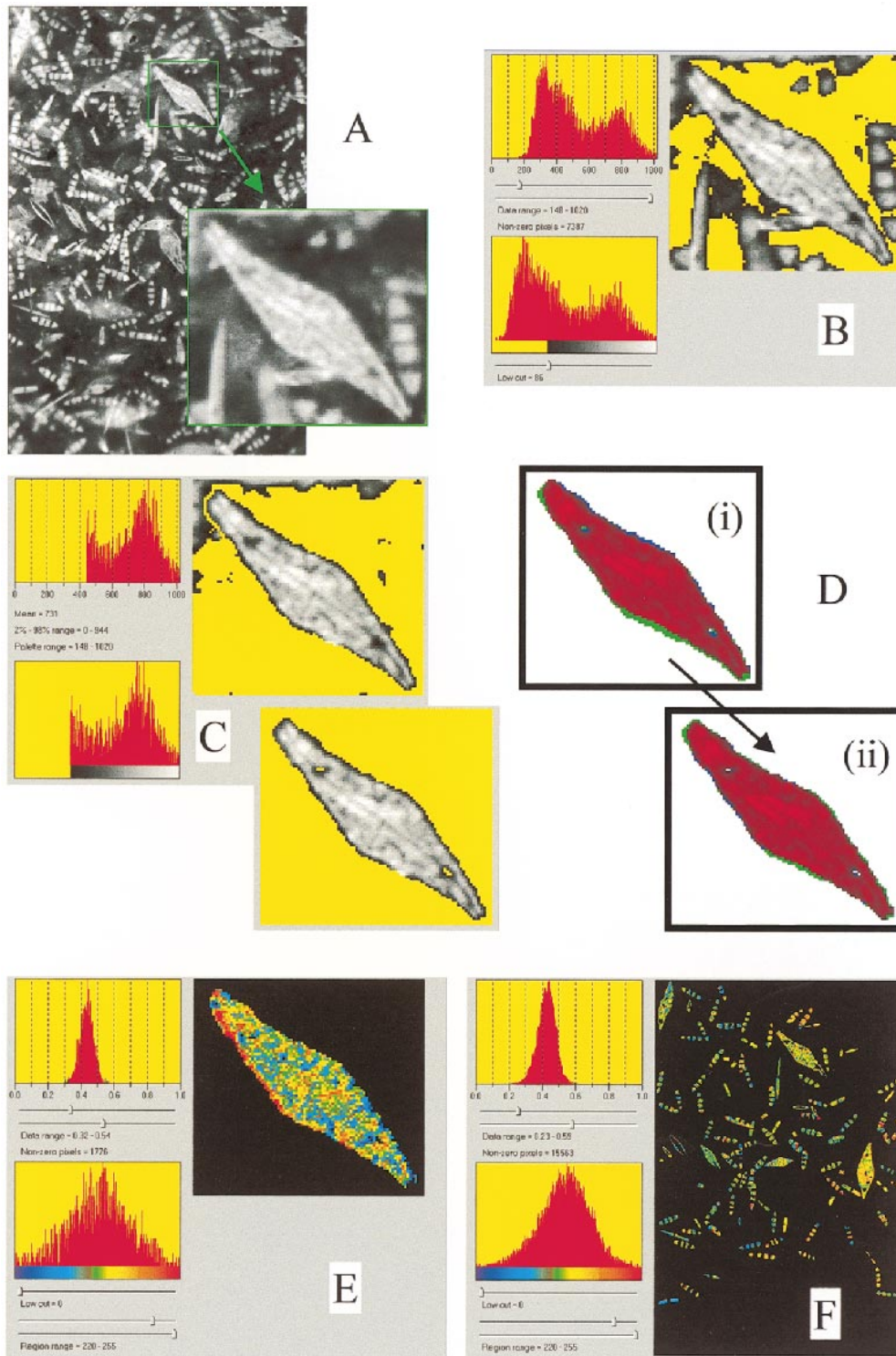


Fig. 1. Method used to determine values of F_q'/F_m' for individual cells within biofilms. Part A shows a grayscale image taken at the F' level of fluorescence through the $40\times$ objective. The inset shows the cell that has been isolated for analysis. Part B shows the first stages of editing that involve the exclusion of low-value pixels using a low-cut filter. Part C shows the cell after the next stage of editing that involves deleting individual pixels and groups of pixels using other editing tools built into the program. Part D(i) shows the F' image of the cell overlapped with the F_m' image of the same cell (isolated in the same way as the F' image). Part D(ii) shows the F' and F_m' images after nudging to improve overlap (red pixels). Part E shows an image of F_q'/F_m' , constructed using the F' and F_m' images in Part D. Values of F_q'/F_m' are only calculated at locations where the F' and F_m' images overlap. Part F shows several isolated cells at their original locations within the F_m' image.

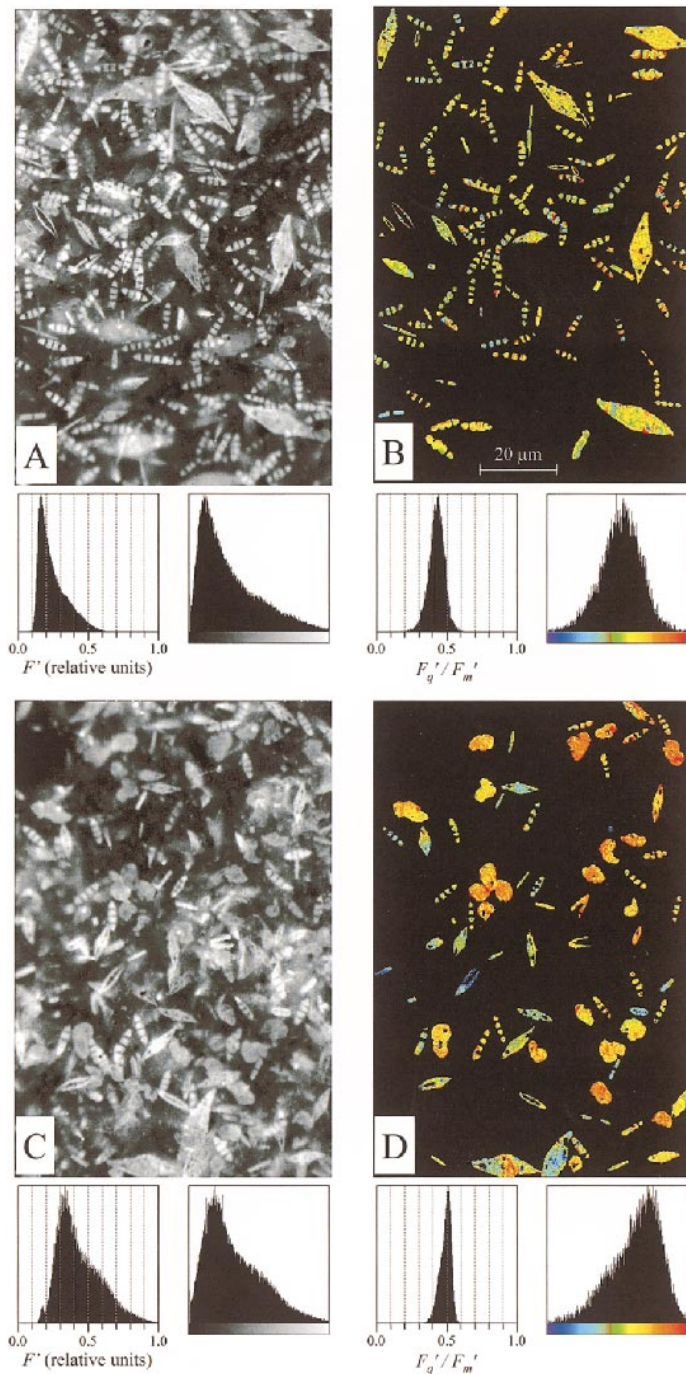


Fig. 2. Low-resolution ($\times 10$ objective), composite images from samples A02 (A and B) and M19 (C and D). These images were used to produce the data in Figs. 4 and 5. A and C are images taken at F_m' . B and D are images of F_q'/F_m' . See Fig. 1 and main text for details of how images B and D were constructed. The frequency histograms with each image show the distribution of values of either F' or F_q'/F_m' (left histogram) and how these values are mapped to the palette (right histogram).

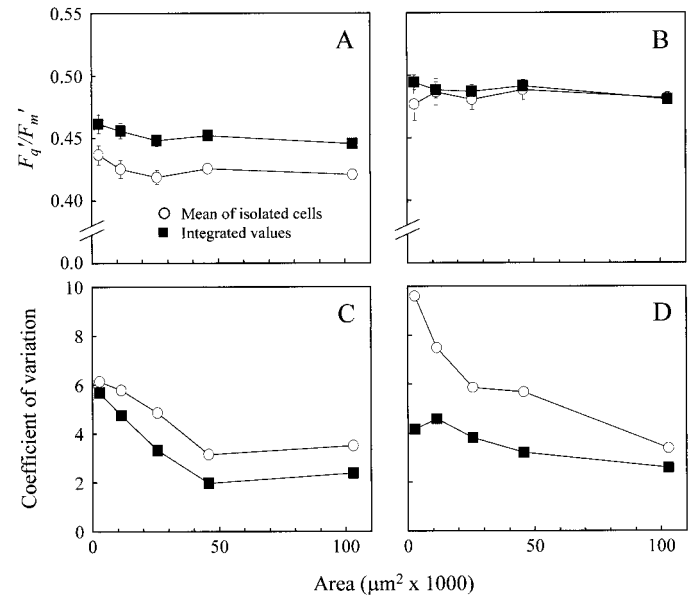


Fig. 3. A and B show the effect of increasing sample area on the mean values of F_q'/F_m' from samples A02 and M19, respectively, while C and D show the effect of increasing sample area on the coefficient of variation from samples A02 and M19, respectively. Points are mean values from all of the cells at the biofilm surface that could be isolated within each quadrat or integrated values from all the pixels within each quadrat.

Euglena species are frequently abundant within cohesive sediments during the summer months (Underwood 1994; Kromkamp et al. 1998), often overlying the epipellic diatoms (Paterson et al. 1998). In this context, the lack of any measurable difference between the two means may be something

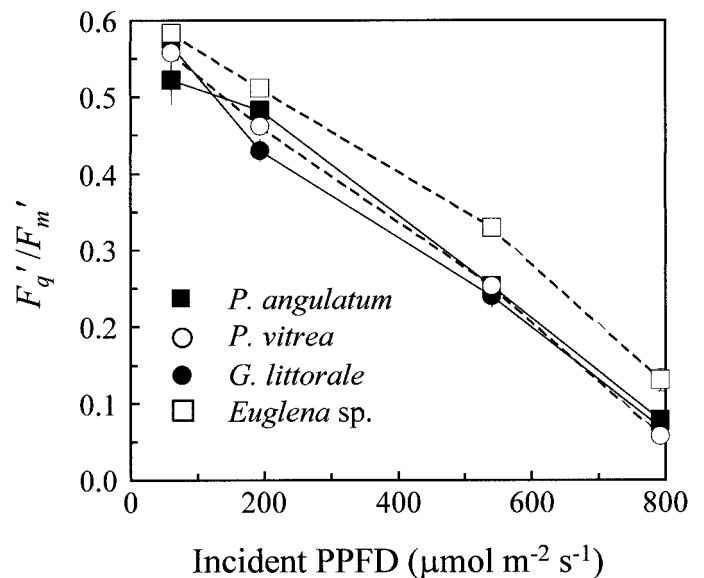


Fig. 4. Light curves for four different taxa within sample M19. Ten cells of each of the four taxa were isolated at each light level from a total of nine images; three images from different regions of each of three subsamples of sample A02. Error bars are shown when these were larger than the data symbols.

of a coincidence; the generally higher F_q'/F_m' values of *Euglena* cells at a particular PPFD, combined with the increased representation of diatoms at depth within the sediment (where PPFD is lower), result in similar values for F_q'/F_m' .

The data in Fig. 4 show values of F_q'/F_m' that were calculated for individual cells of three diatoms (*P. angulatum* [Quekett] W. Smith, *P. vitrea* [W. Smith] Cleve and *G. littorale* [W. Smith] Cleve), and the euglenid, *Euglena* sp. within the same focal plane of sample A02, at four PPFDs between 60 and 790 $\mu\text{mol m}^{-2} \text{s}^{-1}$. For each image, the sample was preilluminated at 790 $\mu\text{mol m}^{-2} \text{s}^{-1}$ for 30 min, and images taken were from the highest to the lowest PPFD used. Ten cells of each of the four taxa examined were isolated from a total of nine images. At the lowest PPFD (60 $\mu\text{mol m}^{-2} \text{s}^{-1}$) all four taxa had similar values of F_q'/F_m' . *Euglena* sp. exhibited values of F_q'/F_m' that were higher than *G. littorale* at 200 $\mu\text{mol m}^{-2} \text{s}^{-1}$ (analysis of variance [ANOVA] < 0.05) and higher than all three diatom taxa at 500 $\mu\text{mol m}^{-2} \text{s}^{-1}$ and 790 $\mu\text{mol m}^{-2} \text{s}^{-1}$ (ANOVA < 0.05). Although these data indicate that absorbed excitation energy is used more efficiently at PS II in cells of *Euglena* sp., at high PPFD, this may simply be due to a lower PS II absorption cross section within these cells and does not necessarily reflect a higher quantum efficiency of incident light use. However, these data do fit well with the dominance of this taxa during summer months (Underwood 1994; Kromkamp et al. 1998). It is clear, from these data, that the system described can be used to resolve relatively subtle differences in the value of F_q'/F_m' among taxa, within an intact system.

Although F_q'/F_m' is a useful parameter, it is not synonymous with primary productivity, the calculation of which requires knowledge of a number of other factors including: the PPFD incident at the surface of the biofilm and the rate at which PPFD decreases with depth; the depth of cells within the sediment; the absorptivity of cells within the sediment; and the efficiency of CO_2 assimilation for individual taxa, calculated through measurement of F_q'/F_m' .

The PPFD at the surface can be monitored using a light meter, while PPFD at depth either can be measured directly using fiberoptic microsensors (Kuhl and Jorgensen 1992, 1994; Underwood and Kromkamp 1999) or determined through calculation, using an extinction coefficient for the sediment. Depth of cells within the sediment can be determined through calibration of the microscope focusing ring or subsequent freezing of sediments and analysis using low temperature scanning electron microscopy (Paterson et al. 1998). Although absorptivity of cells cannot be measured in situ, Hartig et al. (1998) have shown that it is possible to determine values from cultures of isolated cells. Current evidence suggests that the relationship between F_q'/F_m' and ϕ_{CO_2} may be variable among species: although Hartig et al. (1998) observed reasonable linearity between F_q'/F_m' and ϕ_{CO_2} in diatom cultures, data from a number of other algal studies have shown significant deviations from linearity (Falkowski et al. 1986; Kroon 1994; Prášil et al. 1996; Barranguet et al. 1998). Consequently, accurate assessment of primary productivity by different taxa may require that the

nature of the relationship between ϕ_{CO_2} and F_q'/F_m' be determined for each taxa present within a biofilm.

In conclusion, the chlorophyll fluorescence imaging technique described here represents a significant step forward in the development of methods for assessing the contribution of different taxa to the overall level of primary productivity within intact biofilms. The most important feature of this system is the ability to determine the PS II photochemical efficiency through F_q'/F_m' from a large number of individual cells. Translating values of F_q'/F_m' from individual cells to rates of primary production will be a complex process because the attenuation of light with depth, the depth of cells, the absorptivity of cells and the taxa-specific relationships between F_q'/F_m' and ϕ_{CO_2} all have to be taken into account. However, techniques already exist for the measurement of these parameters, and it would seem to be an achievable aim. In addition, it is likely that the ability to measure F_q'/F_m' at the level of individual cells will be of great value in the study of the factors determining the species composition of biofilms under different combinations of environmental conditions.

K. Oxborough¹
A. R. M. Hanlon
G. J. C. Underwood
N. R. Baker

Department of Biological Sciences
University of Essex
Colchester CO4 3SQ, United Kingdom

References

- BARRANGUET, C., J. KROMKAMP, AND J. PEENE. 1998. Factors controlling primary production and photosynthetic characteristics of intertidal microphytobenthos. *Mar. Ecol. Prog. Ser.* **173**: 117–126.
- BLANCHARD, G. F., J. M. GUARINI, P. RICHARD, P. GROS, AND F. MORNET. 1996. Quantifying the short-term temperature effect on light-saturated photosynthesis of intertidal microphytobenthos. *Mar. Ecol. Prog. Ser.* **134**: 309–313.
- DI MARCO, G., F. S. MANES, D. TRICOLI, AND E. VITALE. 1990. Fluorescence parameters measured concurrently with net photosynthesis to investigate chloroplastic CO_2 concentration in leaves of *Quercus ilex* L. *J. Plant Physiol.* **136**: 538–543.
- EDWARDS, G. E., AND N. R. BAKER. 1993. Can CO_2 assimilation in maize leaves be predicted accurately from chlorophyll fluorescence analysis? *Photosynth. Res.* **37**: 89–102.
- FALKOWSKI, P. G., K. WYMAN, A. C. LEY, AND D. C. MAUZERALL. 1986. Relationship of steady-state photosynthesis to fluorescence in eukaryotic algae. *Biochim. Biophys. Acta* **849**: 183–192.
- , D. ZIEMAN, Z. KOLBER, AND P. K. BIENFANG. 1991. Role of eddy pumping in enhancing primary production in the ocean. *Nature* **352**: 55–58.
- GENTY, B., J. M. BRIANTAIS, AND N. R. BAKER. 1989. The relationship between the quantum yield of photosynthetic electron

¹ Corresponding author (koxbor@essex.ac.uk).

Acknowledgments

This work was funded, in part, by NERC grants GR3/11782 and GST/02/1562. A.R.M.H. was funded by a NERC CASE studentship, ref. GT22/96/ENV/D/5.

- transport and quenching of chlorophyll fluorescence. *Biochim. Biophys. Acta* **990**: 87–92.
- HARTIG, P., K. WOLFSTEIN, S. LIPPEMEIER, AND F. COLIJN. 1998. Photosynthetic activity of natural microphytobenthos populations measured by fluorescence (PAM) and ^{14}C -tracer methods: A comparison. *Mar. Ecol. Prog. Ser.* **166**: 53–62.
- KOLBER, Z., AND P. G. FALKOWSKI. 1993. Use of active fluorescence to estimate phytoplankton photosynthesis in situ. *Limnol. Oceanogr.* **38**: 1646–1665.
- KRALL, J. P., AND G. E. EDWARDS. 1990. Quantum yields of photosystem II electron transport and carbon dioxide fixation in C_4 plants. *Aust. J. Plant Physiol.* **17**: 579–588.
- KROMKAMP, J., C. BARRANGUET, AND J. PEENE. 1998. Determination of microphytobenthos PS II quantum efficiency and photosynthetic activity by means of variable chlorophyll fluorescence. *Mar. Ecol. Prog. Ser.* **162**: 45–55.
- KROON, B. M. A. 1994. Variability of photosystem II quantum yield and related processes in *Chlorella pyrenoidosa* (Chlorophyta) acclimated to an oscillating light regime simulating a mixed photic zone. *J. Phycol.* **30**: 841–852.
- KUHL, M., AND B. B. JORGENSEN. 1992. Spectral light measurements in microbenthic phototrophic communities with a fiber-optic microprobe coupled to a sensitive diode-array detector. *Limnol. Oceanogr.* **37**: 1813–1823.
- , AND ———. 1994. The light-field of microbenthic communities—radiance distribution and microscale optics of sandy coastal sediments. *Limnol. Oceanogr.* **39**: 1368–1398.
- MACINTYRE, H. L., R. J. GEIDER, AND D. C. MILLER. 1996. Microphytobenthos: The ecological role of the “secret garden” of unvegetated, shallow-water marine habitats. I. Distribution, abundance and primary production. *Estuaries* **19**: 186–201.
- OLSON, R. J., A. M. CHEKALYUK, AND H. M. SOSIK. 1996. Phytoplankton photosynthetic characteristics from fluorescence induction assays of individual cells. *Limnol. Oceanogr.* **41**: 1253–1263.
- OXBOROUGH, K., AND N. R. BAKER. 1997a. An instrument capable of imaging chlorophyll *a* fluorescence from intact leaves at very low irradiance and at cellular and subcellular levels of organization. *Plant Cell Environ.* **20**: 1473–1483.
- , AND ———. 1997b. Resolving chlorophyll *a* fluorescence images of photosynthetic efficiency into photochemical and non-photochemical components—calculation of qP and Fv'/Fm' without measuring Fo' . *Photosynth. Res.* **54**: 135–142.
- PATERSON, D. M. 1989. Short-term changes in the erodibility of intertidal cohesive sediments related to the migratory behaviour or epipellic diatoms. *Limnol. Oceanogr.* **34**: 223–234.
- , AND OTHERS. 1998. Microbiological mediation of spectral reflectance from intertidal cohesive sediments. *Limnol. Oceanogr.* **43**: 1207–1221.
- PELETIER, H. 1996. Long-term changes in intertidal estuarine diatom assemblages related to reduced input of organic waste. *Mar. Ecol. Prog. Ser.* **137**: 265–271.
- PRAŠIL, O., Z. KOLBER, J. A. BERRY, AND P. G. FALKOWSKI. 1996. Cyclic electron flow around photosystem-II in vivo. *Photosynth. Res.* **48**: 395–410.
- SERÓDIO, J., J. M. DA SILVA, AND F. CATARINA. 1997. Non-destructive tracing of migratory rhythms of intertidal benthic microalgae using in vivo chlorophyll *a* fluorescence. *J. Phycol.* **33**: 542–553.
- SMITH, D. J., AND G. J. C. UNDERWOOD. 1998. Exopolymer production by intertidal epipellic diatoms. *Limnol. Oceanogr.* **43**: 1578–1591.
- UNDERWOOD, G. J. C. 1994. Seasonal and spatial variation in epipellic diatom assemblages in the Severn estuary. *Diatom Res.* **9**: 451–472.
- . 1997. Microalgal colonisation in a saltmarsh restoration scheme. *Estuarine Coastal Shelf Sci.* **44**: 471–481.
- , AND J. KROMKAMP. 1999. Primary production by phytoplankton and microphytobenthos in estuaries. *Adv. Ecol. Res.* **29**: 93–153.
- , C. NILSSON, K. SUNDBÄCK, AND A. WULFF. 1999. Short-term effects of UVB radiation on chlorophyll fluorescence, biomass, pigments and carbohydrate fractions in a benthic diatom mat. *J. Phycol.* **35**: 656–666.
- , M. PHILLIPS, AND K. SAUNDERS. 1998. Distribution of estuarine benthic diatom species along salinity and nutrient gradients. *Eur. J. Phycol.* **33**: 173–183.

Received: 14 October 1999

Accepted: 25 April 2000

Amended: 8 May 2000

On the dispersal of riverine colored dissolved organic matter over the West Florida Shelf

Abstract—We investigated the optical properties of surface water in areas of the West Florida Shelf influenced by riverine discharge and by the occurrence of a phytoplankton plume. Results of absorption and fluorescence spectroscopy analyses and determination of dissolved organic carbon (DOC) concentration showed that the injection of riverine colored dissolved organic matter (CDOM) strongly affected the optical properties and DOC concentrations over the shelf. Riverborne nutrients contributed to an increase in primary productivity. However, during the study period, the increase in primary productivity did not result in the production of significant amounts of CDOM.

Fluorescence spectroscopy results showed that optical prop-

erties of riverine CDOM were lost close to the mouth of the rivers. A simple mathematical model describing mixing between riverine and marine end-members demonstrated that most of the observed changes in optical properties of CDOM along salinity gradients can be explained by mixing. Laboratory mixing experiments between riverine water and seawater indicated that flocculation of organic matter during estuarine mixing did not affect the optical properties of CDOM.

Remote-sensing studies of the Gulf of Mexico using historical data from the Coastal Zone Color Scanner show a recurrent, seasonal chlorophyll bloom over the West Florida Shelf (WFS) every year between February and May (Gilbes